Clinical Infectious Diseases

MAJOR ARTICLE

Understanding the Importance of Contact Heterogeneity and Variable Infectiousness in the Dynamics of a Large Norovirus Outbreak

Jon Zelner,[1] Carly Adams,[2] Joshua Havumaki,[1] and Ben Lopman[2,3]

[1]Department of Epidemiology, University of Michigan School of Public Health, Ann Arbor; and Departments of [2]Epidemiology and [3]Environmental Health, Rollins School of Public Health, Emory University, Atlanta, Georgia

Background. Large norovirus (NoV) outbreaks are explosive in nature and vary widely in final size and duration, suggesting that superspreading combined with heterogeneous contact may explain these dynamics. Modeling tools that can capture heterogeneity in infectiousness and contact are important for NoV outbreak prevention and control, yet they remain limited.

Methods. Data from a large NoV outbreak at a Dutch scout jamboree, which resulted in illness among 326 (of 4500 total) individuals from 7 separate camps, were used to examine the contributions of individual variation in infectiousness and clustered contact patterns to the transmission dynamics. A Bayesian hierarchical model of heterogeneous, clustered outbreak transmission was applied to represent (1) between-individual heterogeneity in infectiousness and (2) heterogeneous patterns of contact.

Results. We found wide heterogeneity in infectiousness across individuals, suggestive of superspreading. Nearly 50% of individual infectiousness was concentrated in the individual's subcamp of residence, with the remainder distributed over other subcamps. This suggests a source-and-sink dynamic in which subcamps with greater average infectiousness fed cases to those with a lower transmission rate. Although the per capita transmission rate within camps was significantly greater than that between camps, the large pool of susceptible individuals across camps enabled similar numbers of secondary cases generated between versus within camps.

Conclusions. The consideration of clustered transmission and heterogeneous infectiousness is important for understanding NoV transmission dynamics. Models including these mechanisms may be useful for providing early warning and guiding outbreak response.

Keywords. norovirus; transmission model; outbreak; MCMC.

Norovirus (NoV) outbreaks are often characterized by explosive dynamics in which many individuals become ill in quick succession. Such outbreaks may rapidly fade out, continue to slowly collect cases, or recrudesce into a second outbreak peak. Such unpredictable and explosive dynamics may indicate superspreading dynamics in which highly infectious individuals account for a disproportionate share of transmission [1]. In addition, contact in outbreak scenarios is likely to be clustered—for example, among patients nested within wards during a nosocomial outbreak, children in classrooms [2], or even animals on farms [3]. Analyses of large NoV outbreaks [4] have noted their wide variation in final size and duration [5, 6] and have strongly suggested that heterogeneous contact combined with superspreading may explain these dynamics.

Despite their importance for NoV outbreak prevention and control, a recent review demonstrated that the set of modeling tools that can capture heterogeneity in contact and infectiousness remains limited [7]. We address this gap by examining the contributions of individual variation in infectiousness and clustered contact patterns to the transmission dynamics of a large, previously published NoV outbreak at a Dutch scout jamboree [8]. This outbreak resulted in illness in more than 300 individuals staying within 7 separate camps within the jamboree. On day 3 of the outbreak, contact precautions and intensive handwashing were implemented. All of the ill individuals were instructed to go to a first-aid tent and were not allowed to aid in the preparation of food until 3 days after their last symptoms had resolved. However, of the 326 observed cases, only 92 visited the first-aid tent and an additional 54 were admitted to a local hospital for rehydration.

Although individuals were exposed to those in other camps, it is likely that a substantial portion of their contacts were concentrated within their assigned camps, where they slept, ate, and spent free time. A prior analysis of these data focused on the evolution of the average infectiousness of cases across all camps. In this paper, we take advantage of the fact that

Received 21 December 2018; editorial decision 9 March 2019; accepted 14 March 2019; published online March 18, 2019.

Correspondence: J. Zelner, Deparment of Epidemiology, University of Michigan School of Public Health, 1415 Washington Heights, Ann Arbor, MI 48109-2029 (jzelner@umich.edu).

Clinical Infectious Diseases® 2020;70(3):493–500

© The Author(s) 2019. Published by Oxford University Press for the Infectious Diseases Society of America. All rights reserved. For permissions, e-mail: journals.permissions@oup.com.

DOI: 10.1093/cid/ciz220

individual time series are available for each subcamp to estimate the rate of within- versus between-camp contact and the evolution of the daily reproduction number, a measure of average infectiousness on each day, within each camp. This allows us to assess whether certain camps likely acted as high-transmission sources of infection that fed cases to lower-incidence camps, or if infectiousness between camps was approximately equivalent, with differences in incidence primarily attributable to stochastic variation.

Sources of Heterogeneous Infectiousness

A key feature of NoV illness is sudden-onset projectile vomiting, which has been suggested to play a key role in NoV outbreaks [9, 10]. The location and timing of these events likely impact the trajectory of an outbreak, because a vomiting event that occurs in public with many individuals nearby may cause many cases [11], whereas one occurring in private may represent a transmission dead end. For example, Wikswo et al [4] documented a large NoV outbreak in which an individual who vomited during boarding of a cruise ship likely infected many passengers at one time. Given an equally significant vomiting event within her own room, such a passenger would likely have had a diminished epidemiologic impact. Similar dynamics have been demonstrated in congregate settings such as restaurants [12] and nursing homes [13]. In addition, persistent environmental contamination following instances of public vomiting may facilitate superspreading by allowing transmission to occur days or weeks after the initial event, even following disinfection [14, 15]. Superspreading can also result from preparation of food served to a large group of individuals (eg, in a restaurant or catering setting) by infectious individuals [16, 17]. Variation in viral shedding may cause some cases to be more infectious on a per-contact basis than those who excrete fewer viral copies per gram of stool or vomitus. However, although rates of viral shedding in stool have been found to be similar in symptomatic and asymptomatic individuals, recent studies suggest that NoV transmission is driven by the vomiting and diarrhea of symptomatic cases [18]. Individuals are likely to have variable contact rates as well. In institutional contexts, such as long-term care facilities or daycare centers, individuals are likely to be clustered into groups, such as wards or classrooms, with varying sizes and within-group contact rates. High-transmission clusters may serve as sources of infection that seed outbreaks in lower-transmission clusters in the same hospital, school, etc. Finally, there is likely to be wide heterogeneity in susceptibility to infection upon exposure to an outbreak. Studies suggest that 10–30% of the population is immune to NoV and will not develop infection even when exposed to a large infectious dose [19–21]. Individuals may also acquire immunity following infection, with protection against reinfection with the same strain and partial immunity to related variants in subsequent seasons [22].

METHODS

In this section, we describe a Bayesian hierarchical model of heterogeneous, clustered NoV outbreak transmission, which we apply to the previously published NoV outbreak data from a large scout jamboree in the Netherlands in 2004 [8]. Figure 1A shows the distribution of the 326 cases on each day of the outbreak; Figure 2 shows the evolution of the outbreak within the 7 individual camps. We build on the framework for representing between-individual heterogeneity in infectiousness from Lloyd-Smith et al [1] to represent (1) between-individual heterogeneity in infectiousness and (2) heterogeneous patterns of contact.

Transmission Model

In this section, we outline a stochastic, discrete-time model of NoV transmission within and between subcamps involved in the outbreak. This model is similar to the susceptible-exposed-infectious-recovered (SEIR) models applied to NoV transmission [23, 24], with key modifications to accommodate between-individual variability in infectiousness. We extended the framework in Lloyd-Smith et al [1] to modeling individual-level heterogeneity in within-camp infectiousness as well as interaction between units. We denote the number of incident cases observed on day t in camp j to be y_{jt} and the unobserved number of infections on day t in camp j as y^*_{jt}. These values are different because of the latent period between infection and onset of symptoms. Individuals are assumed to be infectious at the beginning of their day of onset. We denote the day of onset of disease for individual i as z_i.

Individual-level Variation in Infectiousness

We assume that the expected number of secondary cases generated by each case varies across individuals but that the proportion of secondary cases within the individual's camp, denoted as ζ, is constant across individuals. We denote R as the average number of secondary infections generated by each case, with $R_W = \zeta R$ equal to the number of secondary infections the individual would generate in his camp if he were the first infectious case and $R_B = R(1-\zeta)$ the number of cases he would generate in all other camps.

Each case is assumed to have an individual reproduction number r_i drawn from a gamma distribution with shape parameter R_k and a scale parameter R_θ. So, $r_i \sim Gamma(R_k, R_\theta)$, and population mean value $R = R_k * R_\theta$. However, because within each camp multiple cases may become infectious on a given day, the value of r_i for each case is not identifiable. Nevertheless, we can take advantage of the fact that the sum of n gamma-distributed variables with shape k and scale θ is gamma distributed with shape parameter nk and scale θ to sample values r_{jt}, indicating the daily total force of infection from all incident cases in camp j on day t (denoted as y_{jt}), so that $\lambda_{jt} \sim Gamma(y_{jt}R_k, R_\theta)$.

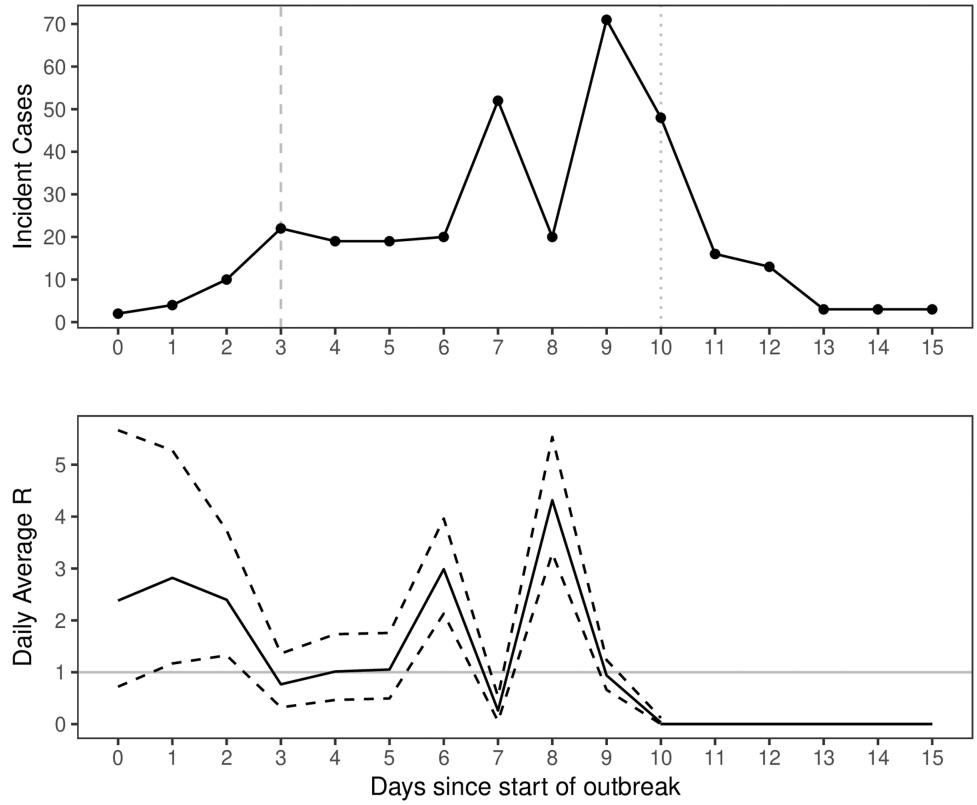

Figure 1. *A,* Number of new cases per day. The dashed vertical line indicates the beginning of hygiene interventions; the dotted line indicates the end of the jamboree. *B,* Estimated daily average reproductive number across all camps. Dashed lines indicate 95% posterior credible intervals. The horizontal gray line indicates a critical value of $R = 1$.

Infectiousness as a Function of Time Since Symptom Onset

We follow the approach to modeling the change in individual infectiousness after symptom onset described in Cauchemez and Ferguson [25] and previously applied to NoV in Zelner et al [24]. In this framework, a probability mass function is used to model the proportion of an individual's infectiousness occurring on each day following symptom onset (including day of onset). In the current model, we allow individual infectiousness to decay according to a geometric distribution with parameter $\gamma \in (0, 1]$, where $g(x|\gamma) = \gamma(1-\gamma)^x$.

When $t \geq z_i$, $g(t - z_i)$ is the proportion of the infectiousness of individual i deposited on day t. When $t < z_i$, this value is equal to zero (ie, before the individual becomes infectious). The parameter γ has a straightforward interpretation as the proportion of the individual's infectiousness deposited on the day of symptom onset and the proportion of remaining infectiousness deposited each day thereafter.

Force of Infection

Accounting for individual infectiousness, r_i, and the proportion of infectiousness each case deposits within his camp, ζ, we can write the force of infection within each camp at each time, t, as follows:

$$\lambda_{jt} = \sum_{k \leq t} g(t-k) \left(\frac{\zeta r_{jk}}{n_j} + (1-\zeta) \sum_{i \neq j} \frac{r_{ik}}{(N - n_i)} \right)$$

The risk of infection posed by each case to individuals in the other camps is a function of the size of the population outside his or her camp—that is, $N - n_j$ for an individual residing in camp j.

Latent Period

We utilize previous estimates of the distribution of NoV incubation period duration [26] that assume a log-normal distribution, with a median incubation time of 1.2 days (95% confidence interval [CI], 1.2–1.3 days) and a dispersion factor (corresponding to the variance of the underlying normal distribution) of 1.56 (95% CI, 1.49–1.62). In practice, this means that 95% of cases will become symptomatic within 2.5 days of infection (95% CI, 2.4–2.6 days). We use a discrete approximation to this value, where $g(x|\eta)$ is the probability mass function of the geometric distribution, where $\eta = 0.8$ is the probability of manifesting symptoms on each day following infection, for an average latent period of approximately 1.2 days. For a full

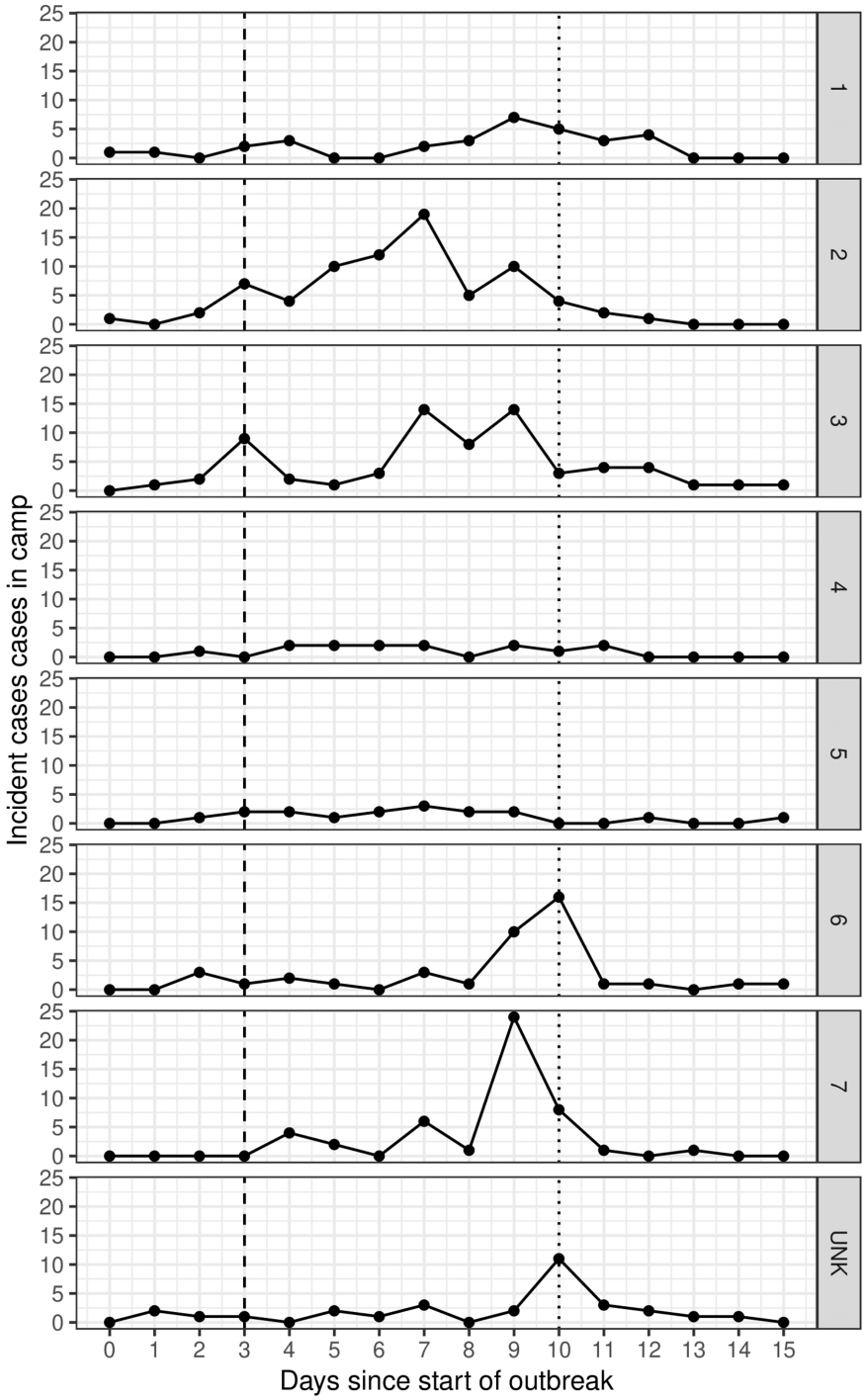

Figure 2. Number of incident cases in each camp by day of outbreak. The dashed vertical line indicates the beginning of hygiene interventions; the dotted vertical line indicates the end of the jamboree. Abbreviation: UNK, cases with unknown camp assignment.

description of the likelihood function used to fit the model, see the Supplementary Methods.

Missing Data

Although the outbreak data are notable for their detail on contact, camp assignments are unknown for 30 out of the 326 cases (9%) (see Figure 1). The majority (n = 18) of these missing cases occurred on or after the final day of the jamboree, likely making their impact on overall outbreak size minimal. However, to account for the potential effect of these cases on estimates of the infectiousness of cases observed on prior days of the outbreak, we created 20 random datasets with these unobserved cases distributed uniformly at random across the camps. The model was then fit to each of these augmented datasets, and the posterior distributions

obtained from 20 augmented datasets were combined into a single distribution that reflects uncertainty in these case assignments. This is analogous to a weighting scheme in which each input dataset is assigned an equal sampling weight.

RESULTS

Average and Individual-level Infectiousness

The average reproduction number $R = 1.15$ (95% Credible Interval [CrI] = 0.73, 1.94). The value of r_i across individuals is highly dispersed, $\alpha = 0.04$ (95% CrI = 0.02, 0.07), corresponding to a standard deviation of $\sigma_R = 5.89$ (95% CrI = 3.58, 13.67), indicating wide heterogeneity in infectiousness across individuals. This suggests a superspreading dynamic, because the median value of r_i is near zero and 90% (95% CrI = 85%, 90%) of cases had $r_i < 1$, with a small number of cases responsible for most of the disease burden. For each case, approximately $\zeta = 0.53$ (95% CrI = 0.46, 0.61) of secondary infections (eg, $\zeta * r_i$) occurred within his subcamp, suggesting that the infection risk posed to same-camp contacts was approximately 6 times greater than for contacts in other subcamps. Almost all infectiousness was concentrated on the day of onset, as indicated by the parameter estimate $\gamma = 0.97$ (95% CrI = 0.93, 0.99). These results echo the finding from Zelner et al [24], which found a strong concentration of individual infectiousness on the day of illness onset. Table 1 contains parameter estimates and 95% posterior credible intervals for key parameters.

Figure 3 shows the evolution of $\bar{r}_t$ across all camps over the course of the outbreak. This suggests a pattern in which average infectiousness was indeed reduced in the period following the onset of interventions on day 3 of the outbreak, but with a number of large transmission events several days after the implementation of intensive hygiene interventions. Figure 1B shows the total force of infection (ie, within-camps + between camp) for each day of the outbreak, λ_{jt}. Notably, transmission within each camp except for camp 2 is characterized by a combination of sporadic superspreading events and very low transmission, rather than a time-constant rate of infectiousness. In camp 2, the total infectiousness is approximately constant for the first 6 days of the outbreak, reflecting the large overall burden of illness in that camp and suggesting that it was driven largely by endogeneous transmission.

Between- Versus Within-camp Transmission

The parameter ζ indicates the total proportion of infections expected to be generated within versus between camps. To understand how the contributions of individual camps to the overall outbreak vary, we can disaggregate this value to estimate the proportion of infection occurring within each camp, which we denote as ζ_j. To do this, we calculated the proportion of the total force of infection experienced in each camp over all days of the outbreak that was attributable to within-camp exposure, as follows:

$$\zeta_j = \sum_{t=0}^{T} \frac{\lambda_{jt}^W}{\lambda_{jt}^B + \lambda_{jt}^W}.$$

Figure 4 illustrates the variation in the proportion of infection acquired within versus between camps as a function of the total outbreak incidence accounted for by that camp. The figure suggests a source-and-sink pattern in which endogenous transmission in high-incidence camps (camps 2 and 3) fed cases into the medium (camps 1, 6, and 7) and low-incidence (camps 4 and 5) camps.

DISCUSSION

Our results suggest that the per capita transmission rate within camps was significantly greater than between camps, because cases generated approximately as many secondary cases in camps other than their own while the pool of susceptible individuals in other camps was approximately 6 times greater than within camp for each case. The wide heterogeneity in average infectiousness across camps suggests a source-and-sink dynamic in which camps with greater average infectiousness fed cases into those with a lower average transmission rate. These results suggest that developing tools to identify and target interventions in high-transmission subpopulations may be useful for minimizing NoV outbreak risk. In addition, the wide variation in individual infectiousness suggests that the daily hazard of infection in outbreak data may only be weakly linearly related to the number of incident cases in the population on that day.

It is important to note how our estimates of infectiousness evolution over time from all camps differ from those presented by Heijne et al [8]. This may be attributable to key differences in model structure. For example, our model shows an early peak in infectiousness on the second day of the outbreak, whereas in the prior analysis the largest peak occurred on the first day. This may result from the fact that our model uses an explicit representation of the latent period, which imposes a delay between infection and infectiousness, rather than a generation-time approach.

Table 1. Model Parameters and Their Estimated Posterior Median Values and 95% Posterior Credible Intervals

Parameter	Definition	Estimate (95% Credible Interval)
γ	Proportion of infectiousness each day	0.97 (.93–.99)
R	Average individual reproduction number	1.15 (.73–2.20)
ζ	Proportion of infections within camp	0.53 (.44–.61)
α	Dispersion of case-level infectiousness	0.04 (.02–.07)

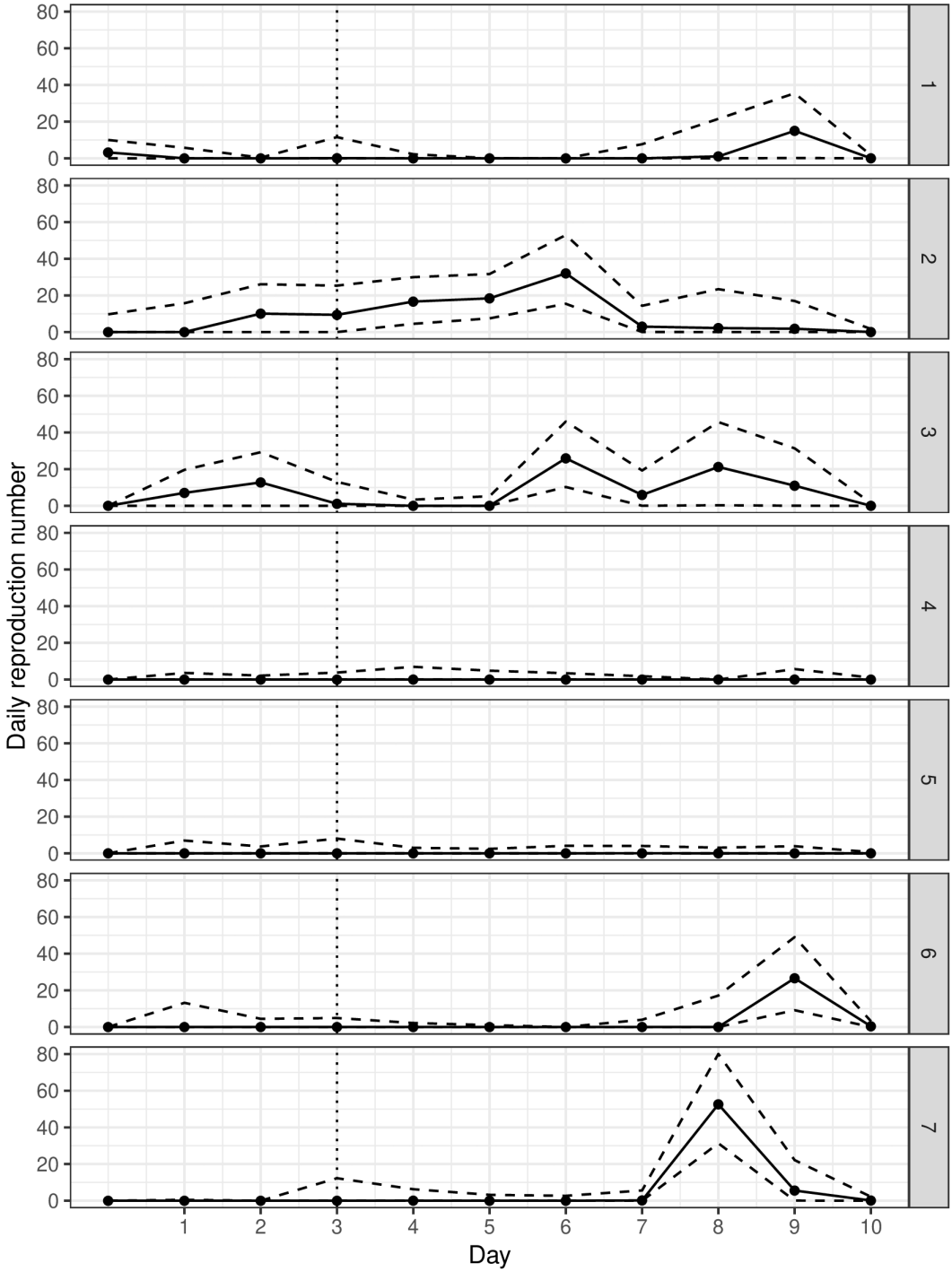

Figure 3. Estimated daily average reproductive number for each camp. The vertical dotted line indicates the beginning of the hygiene interventions. Dashed lines indicate 95% posterior credible intervals.

Our model also demonstrates 2 peaks of infectiousness on days following implementation of interventions, whereas the model in Heijne et al [8] shows a pattern of declining average infectiousness during this period. This may be attributable to the fact that our model accounts for susceptible depletion over the course of the outbreak, which reduces the number of individuals available to infect and necessarily reduces the effective reproduction number, which measures the number of realized infections. Since our model captures infection potential (ie, the expected number of secondary infections on the first day of the outbreak), peaks in the average infectiousness of secondary cases are more readily detectable. In addition, the inclusion of differential rates of contact within and between camps may have impacted estimates of the time course of infectiousness.

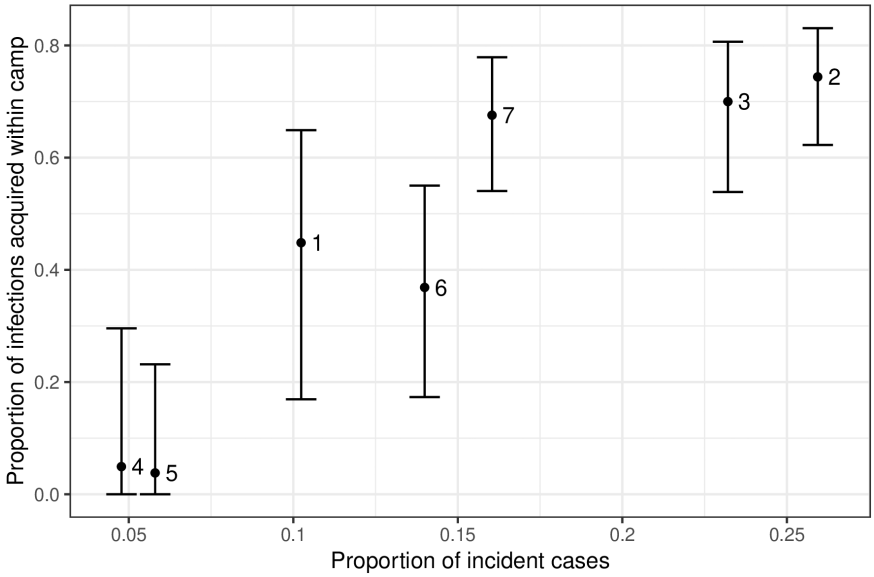

Figure 4. The proportion of infections acquired within camp, as a function of the total proportion of incident cases within that camp. Points indicate posterior medians; vertical bars indicate 95% posterior credible intervals. Each point is labeled by the camp in Figure 2 to which it corresponds.

Our analysis has several limitations. The missingness of camp assignments for approximately 9% of cases may impact our estimates of within- and between-camp infectiousness. However, a comparison of results obtained by integrating over 20 augmented datasets and the raw data in which cases with missing camp assignments were dropped had no impact on our qualitative or quantitative results. This is likely because most of these cases occurred at the end of the outbreak, minimizing contact. In addition, although our model highlights transmission heterogeneity not explicitly modeled in an earlier analysis of these data, it is not possible from the present analysis to suggest that this model has better predictive properties. A formal model comparison, which is outside the scope of this analysis, would be important for assessing the relative utility of different outbreak models for predicting both the burden and tempo of NoV outbreaks. In addition, the original analysis by Heijne et al [8] identified multiple circulating NoV genotypes, suggesting that not all cases belonged to the same transmission cluster. Because genotyping was performed on only a subset of cases in the original outbreak, such information was not available for this analysis. However, the inclusion of pathogen genetic data in future outbreak studies would likely result in reduced uncertainty regarding transmission rates and infection sources.

The present analysis may also contribute useful tools for modeling future NoV outbreaks as well as of other pathogens characterized by large amounts of heterogeneity in transmission. Although the data were aggregated to daily counts of incident cases, we were able to estimate between-individual variation in infectiousness because the sum of gamma-distributed random variables is also gamma distributed. This framework may be useful for modeling heterogeneity in transmission in other contexts as well, because daily or weekly counts are commonplace in outbreak data.

Because these data did not contain information on discrete instances of public vomiting, it is not possible to test the hypothesis that such events contributed to the wide variation in infectiousness found in these data. However, our results suggest that collection of data on the timing and location of potential superspreading events could be helpful for predicting the evolution of an outbreak and allowing models to be used as aids for real-time targeting of interventions to slow or halt transmission in an emerging outbreak. However, it is important to note that for modeling tools such as the one described here to be truly useful for outbreak response, they need to be both optimized for prediction of the epidemic trajectory and likely intervention effects and packaged as software that can readily be used in the context of an evolving outbreak response, similar to the population spatiotemporal cluster-detection tool *SatScan* [27].

Supplementary Data

Supplementary materials are available at *Clinical Infectious Diseases* online. Consisting of data provided by the authors to benefit the reader, the posted materials are not copyedited and are the sole responsibility of the authors, so questions or comments should be addressed to the corresponding author.

Notes

Financial support. J. Z. was funded by a grant from the rOpenSci Foundation. B. L. was funded by National Institutes of Health/National Institute of General Medical Sciences (grant number R01 GM124280), and B. L. and C. A. were supported by the Agency for Healthcare Research and Quality (grant number R01 HS025987).

Potential conflicts of interest. B. L. received support from Takeda Pharmaceutical, Centers for Disease Control and Prevention Foundation, and Hall Booth Smith, P.C., unrelated to the submitted work. All other authors have no other potential conflicts of interest to declare. All authors have submitted the

ICMJE Form for Disclosure of Potential Conflicts of Interest. Conflicts that the editors consider relevant to the content of the manuscript have been disclosed.

References

1. Lloyd-Smith JO, Schreiber SJ, Kopp PE, Getz WM. Superspreading and the effect of individual variation on disease emergence. Nature **2005**; 438:355–9.
2. Cauchemez S, Bhattarai A, Marchbanks T, et al. Role of social networks in shaping disease transmission during a community outbreak of 2009 H1N1 pandemic influenza. Proc Natl Acad Sci USA **2011**; 108:2825–30.
3. Haydon DT, Chase-Topping M, Shaw DJ, et al. The construction and analysis of epidemic trees with reference to the 2001 UK foot-and-mouth outbreak. Proc Biol Soc **2003**; 270:121–7.
4. Wikswo ME, Cortes J, Hall AJ, et al. Disease transmission and passenger behaviors during a high morbidity norovirus outbreak on a cruise ship, January 2009. Clin Infect Dis **2011**; 52:1116–22.
5. Matthews JE, Dickey BW, Miller RD, et al. The epidemiology of published norovirus outbreaks: a review of risk factors associated with attack rate and genogroup. Epidemiol Infect **2012**; 140:1161–72.
6. Bitler EJ, Matthews JE, Dickey BW, Eisenberg JN, Leon JS. Norovirus outbreaks: a systematic review of commonly implicated transmission routes and vehicles. Epidemiol Infect **2013**; 141:1563–71.
7. Gaythorpe KAM, Trotter CL, Lopman B, Steele M, Conlan AJK. Norovirus transmission dynamics: a modelling review. Epidemiol Infect **2018**; 146:147–58.
8. Heijne JC, Teunis P, Morroy G, et al. Enhanced hygiene measures and norovirus transmission during an outbreak. Emerg Infect Dis **2009**; 15:24–30.
9. O'Neill PD, Marks PJ. Bayesian model choice and infection route modelling in an outbreak of Norovirus. Stat Med **2005**; 24:2011–24.
10. Cheesbrough JS, Green J, Gallimore CI, Wright PA, Brown DW. Widespread environmental contamination with Norwalk-like viruses (NLV) detected in a prolonged hotel outbreak of gastroenteritis. Epidemiol Infect **2000**; 125:93–8.
11. Marks PJ, Vipond IB, Regan FM, Wedgwood K, Fey RE, Caul EO. A school outbreak of Norwalk-like virus: evidence for airborne transmission. Epidemiol Infect **2003**; 131:727–36.
12. Marks PJ, Vipond IB, Carlisle D, Deakin D, Fey RE, Caul EO. Evidence for airborne transmission of Norwalk-like virus (NLV) in a hotel restaurant. Epidemiol Infect **2000**; 124:481–7.
13. Petrignani M, van Beek J, Borsboom G, Richardus JH, Koopmans M. Norovirus introduction routes into nursing homes and risk factors for spread: a systematic review and meta-analysis of observational studies. J Hosp Infect **2015**; 89:163–78.
14. Jones EL, Kramer A, Gaither M, Gerba CP. Role of fomite contamination during an outbreak of norovirus on houseboats. Int J Environ Health Res **2007**; 17:123–31.
15. Repp KK, Keene WE. A point-source norovirus outbreak caused by exposure to fomites. J Infect Dis **2012**; 205:1639–41.
16. Kuritsky JN, Osterholm MT, Greenberg HB, et al. Norwalk gastroenteritis: a community outbreak associated with bakery product consumption. Ann Intern Med **1984**; 100:519–21.
17. de Wit MA, Widdowson MA, Vennema H, de Bruin E, Fernandes T, Koopmans M. Large outbreak of norovirus: the baker who should have known better. J Infect **2007**; 55:188–93.
18. Teunis PF, Sukhrie FH, Vennema H, Bogerman J, Beersma MF, Koopmans MP. Shedding of norovirus in symptomatic and asymptomatic infections. Epidemiol Infect **2015**; 143:1710–7.
19. Lindesmith L, Moe C, Marionneau S, et al. Human susceptibility and resistance to Norwalk virus infection. Nat Med **2003**; 9:548–53.
20. Kambhampati A, Payne DC, Costantini V, Lopman BA. Host genetic susceptibility to enteric viruses: a systematic review and metaanalysis. Clin Infect Dis **2016**; 62:11–8.
21. Nordgren J, Sharma S, Kambhampati A, Lopman B, Svensson L. Innate resistance and susceptibility to norovirus infection. PLoS Pathog **2016**; 12:e1005385.
22. Rouhani S, Penataro Yori P, Paredes Olortegui M, et al. Norovirus infection and acquired immunity in 8 countries: results from the mal-ed study. Clin Infect Dis **2016**; 62:1210–7.
23. Zelner JL, King AA, Moe CL, Eisenberg JN. How infections propagate after point-source outbreaks: an analysis of secondary norovirus transmission. Epidemiology **2010**; 21:711–8.
24. Zelner JL, Lopman BA, Hall AJ, Ballesteros S, Grenfell BT. Linking time-varying symptomatology and intensity of infectiousness to patterns of norovirus transmission. PLoS One **2013**; 8:e68413.
25. Cauchemez S, Ferguson NM. Methods to infer transmission risk factors in complex outbreak data. J R Soc Interface **2012**; 9:456–69.
26. Lee RM, Lessler J, Lee RA, et al. Incubation periods of viral gastroenteritis: a systematic review. BMC Infect Dis **2013**; 13:446.
27. Greene SK, Peterson ER, Kapell D, Fine AD, Kulldorff M. Daily reportable disease spatiotemporal cluster detection, New York City, New York, USA, 2014-2015. Emerg Infect Dis **2016**; 22:1808–12.